International Journal of Engineering & Technology, 7 (4.10) (2018) 1059-1069

International Journal of Engineering & Technology

Website: www.sciencepubco.com/index.php/IJET

Research paper

Flow of a Jeffrey Fluid Between Two Long Vertical Thin Plates with Porous Medium

S. Sreenadh[1], B. Govindarajulu[2], A.N.S. Srinivas[3*] and R. Nageshwar Rao[4]

[1] Department of Mathematics, Sri Venkateswara University, Tirupati, 517 502, A.P., India.
[2]Department of Mathematics, Sri Venkateswara Arts College, Tirupati, 517 502, A.P., India.
[3, 4] Department of Mathematics, School of Advanced Sciences, VIT, Vellore, 632 014, T.N., India.
**Corresponding author E-mail: anssrinivas@vit.ac.in*

Abstract

The present study investigates fully developed free - convection Jeffrey fluid flow between two vertical plates with porous medium. The vertical plates are moving with same velocity but in opposite directions. The coupled nonlinear governing equations are solved by using the linearization technique. The solutions for velocity distribution, temperature distribution, skin friction and rate of heat transfer is obtained in the presence of porous medium by Iterative procedure. Shooting technique with Runge - Kutta method of order four is proposed to compare the numerical results for velocity and temperature distribution. The numerical results obtained by both methods are compared and presented graphically. It is observed that an increase in the permeability parameter causes decrease in the fluid velocity and an increase in the Jeffrey fluid parameter causes an enhancement in the fluid velocity. The significance of various pertinent parameters like Grashof number, Prandtl number, Eckert number and the plate velocity are explained through graphs.

Keywords: *Free convection; Heat transfer; Vertical plates; Jeffrey parameter.*

1. Introduction:

In recent times various researchers give importance in the wide applications of free convection flow with heat transfer applications in melt spinning, glass-fibre production processes, food processing, mechanical forming processes etc. The study of Convective flow phenomenon has significant applications in various fields such as groundwater hydrology, coal combustors, electronic systems cooling and geothermal energy extraction etc. The pioneering theoretical work has been done by Ostrach [1]. The Grashof number plays a significant role in affecting the fluid flow in free and forced convection with heat transfer characteristics.

The effect of the Grashof number has been studied in the past, both when it is large and small. The effect of Grashof number on laminar flow of free convection with heat transfer was examined by Suriano et al., [2]. The viscous fluid flow through a porous wall with convective acceleration was discussed by Yamamoto and Yoshida [3]. Vajravelu [4] analyzed free convection flow with heat transfer effects. A model to understand the flow between two permeable beds is presented by Sreenadh and Arunachalam [5].

The velocity and temperature distributions in both porous and non-porous regions were studied by many researchers. Rajagopal [6] studied the non-Newtonian fluid flow past an infinite porous plate. The peristaltic flow of a Jeffrey fluid through avertical porous stratum with heat transfer effects was investigated by Vajravelu et al., [7]. Umavathi and Shekar [8] examined the unsteady flow and heat transfer in a vertical corrugated channel containing a porous and viscous fluid region. Heat transfer flow through a porous medium bounded by an infinite vertical plate with magnetic field was studied by Raptis et al., [9]. Free flow of a Jeffrey fluid between two long vertical thin plates studied was by Srinivas et al., [10].

Motivated by this, we proposed to study free convection and heat transfer influence on Jeffrey fluid flow with porous medium confined between two long, parallel, vertical plates moving with same velocities but in opposite directions. The solutions for velocity distribution, temperature distribution, skin friction and rate of heat transfer are obtained by using Iterative procedure. Shooting technique with Runge -Kutta method of order four is proposed to compare the numerical results for velocity and temperature distribution. The numerical results obtained by both methods are compared and presented graphically.

2. Mathematical Formulation:

Consider fully developed free - convection Jeffrey fluid flow between two vertical plates with porous medium is shown in Figure 1. Let X–axis is considered along the plates in the upward direction and Y–axis along the distance between the plates. Let the end conditions be neglected with the foregoing assumptions we may take the flow field and the temperature field as

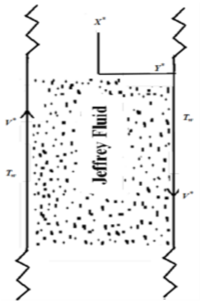

Fig. 1: Physical Model

$$U = U(Y) \tag{1}$$
$$Y = 0$$
$$W = 0$$
$$T = T(Y) \tag{2}$$

The governing equations are

$$\frac{d^2U}{dY^2} - \frac{1+\lambda_1}{\mu}\left(\frac{dP}{dX}\right) - \frac{\rho(1+\lambda_1)}{\mu} g_x - \frac{U}{K} = 0 \tag{3}$$

$$\frac{dP}{dY} = 0 \tag{4}$$

$$\frac{d^2T}{dY^2} + \frac{\mu}{(1+\lambda_1)k}\left(\frac{dU}{dY}\right)^2 = 0 \tag{5}$$

Where ρ is the density, P is the pressure, μ is the coefficient of viscosity, k is the thermal conductivity, g_x is the acceleration due to gravitation and λ_1 is the Jeffrey parameter. The equation of continuity having been satisfied identically. By using the Boussinesq approximation, namely $\frac{\rho - \rho_s}{\rho} = -\beta(T - T_s)$ for the density in Eq. (3) and making similar simplification as in reference [1], we rephrase equations (3) - (5) as

$$\frac{d^2U}{dY^2} + \frac{(1+\lambda_1)\rho g_x \beta}{\mu}(T - T_s) - \frac{U}{K} = 0 \tag{6}$$

$$\frac{d^2T}{dY^2} + \frac{\mu}{(1+\lambda_1)k}\left(\frac{dU}{dY}\right)^2 = 0 \tag{7}$$

Boundary conditions of the problem are

$$\begin{aligned} &Y = 0: \; U = V^*; \; T = T_w \\ &Y = d: \; U = -V^*; \; T = T_w \end{aligned} \tag{8}$$

Introducing the non-dimensional variables

$$y = \frac{Y}{d}; u = \frac{U d}{v}; v = \frac{V^* d}{v}; \theta = \frac{T - T_s}{T_w - T_s}; \sigma = \frac{d}{\sqrt{K}}$$

Into equations (6), (7) and the boundary conditions (8), we obtain

$$\frac{d^2u}{dy^2} + (1+\lambda_1)G\theta - \sigma^2 u = 0 \tag{9}$$

$$\frac{d^2\theta}{dy^2} + \frac{PE}{(1+\lambda_1)}\left(\frac{du}{dy}\right)^2 = 0 \tag{10}$$

$$\begin{aligned} &u = V, \theta = 1 \quad at \quad y = 0 \\ &u = -V, \theta = 1 \; at \quad y = 1 \end{aligned} \tag{11}$$

Where $G = \frac{d^3 g_x \beta (T_w - T_s)}{v^2}, E = \frac{v^2}{d^2 C_p (T_w - T_s)}, P = \frac{\mu C_p}{k}$.

3. Numerical Methods:

In order to solve the non–linear boundary value problem of equations (9) and (10) subject to the conditions (11), we have taken two different methods, namely, an iterative procedure as given by Ostrach [1] and a Shooting method with Runge –Kutta method of order four. The methods are described as follows:

3.1. Iterative Procedure:

To solve the non–linear boundary value problem, the equations (9) and (10) subject to the conditions (11) we define an iterative procedure Ostrach [1] as

$$\frac{d^2u_i}{dy^2} + (1+\lambda_1)G\theta_i - \sigma^2 u_i = 0 \tag{12}$$

$$\frac{d^2\theta_i}{dy^2} + \frac{PE}{(1+\lambda_1)}\left(\frac{du_{i-1}}{dy}\right)^2 = 0 \tag{13}$$

$$\begin{aligned} &u_i = V, \theta_i = 1 \quad \text{at} \quad y = 0 \\ &u_i = -V, \theta_i = 1 \; \text{at} \quad y = 1 \end{aligned} \tag{14}$$

Initially $u_0 = 0$ for $i \geq 1$, then we write the solution as

$$u_1 = B_1 e^{-s\sigma y} + B_2 e^{s\sigma y} + \frac{G}{\sigma^2} \tag{15}$$

$$\theta_1 = 1 \tag{16}$$

$$\begin{aligned} u_2 = {} & F_1 e^{-\sigma sy} + F_2 e^{\sigma sy} + \frac{G_1}{3\sigma^2 s^2} e^{-2\sigma sy} + \frac{G_2}{3\sigma^2 s^2} e^{2\sigma sy} - \frac{G_3}{\sigma^2 s^2} y^2 \\ & - \frac{G_4}{\sigma^2 s^2} y - \left(\frac{G_5}{\sigma^2 s^2} + \frac{2G_3}{\sigma^4 s^2}\right) \end{aligned} \tag{17}$$

$$\theta_2 = D_1 e^{-2\sigma sy} + D_2 e^{2\sigma sy} + D_3 y^2 + D_4 y + D_5 \tag{18}$$

$$\begin{aligned} u_3 = {} & P_1 e^{-s\sigma y} + P_2 e^{s\sigma y} + P_3 e^{-4s\sigma y} + P_4 e^{-3s\sigma y} + P_5 e^{-2s\sigma y} \\ & - P_6 y e^{-s\sigma y} + P_7 e^{4s\sigma y} + P_8 e^{3s\sigma y} + P_9 e^{2s\sigma y} + P_{10} y e^{s\sigma y} \\ & + P_{11} e^{-2s\sigma y}\left(y - \frac{4}{3s\sigma}\right) - P_{12} e^{-s\sigma y}\left(\frac{y^2}{2} + \frac{y}{2s\sigma}\right) + P_{13} e^{2s\sigma y}\left(y + \frac{4}{3s\sigma}\right) \\ & + P_{14} e^{s\sigma y}\left(\frac{y^2}{2} - \frac{y}{2s\sigma}\right) - P_{15} y^4 - P_{16} y^3 - P_{17} y^2 - P_{18} y - P_{19}. \end{aligned} \tag{19}$$

$$\begin{aligned} \theta_3 = {} & N_1 e^{-4s\sigma y} + N_2 e^{-3s\sigma y} + e^{-2s\sigma y}(N_3 + N_{10}) + e^{-s\sigma y}(N_4 + N_{12}) \\ & + N_5 e^{4s\sigma y} + N_6 e^{3s\sigma y} + e^{2s\sigma y}(N_7 - N_{14}) + e^{s\sigma y}(N_8 - N_{16}) \\ & + N_9 y e^{-2s\sigma y} + N_{11} y e^{-s\sigma y} + N_{13} y e^{2s\sigma y} + N_{15} y e^{s\sigma y} \\ & + N_{17} y^4 + N_{18} y^3 + N_{19} y^2 + M_1 y + M_2. \end{aligned} \tag{20}$$

3.1.1. Shear Stress:

The dimensionless shear stress is given by

$$\begin{aligned} \tau = {} & \frac{du}{dy} \\ = {} & -s\sigma p_1 e^{-s\sigma y} + s\sigma p_2 e^{-2s\sigma y} - 4s\sigma p_3 e^{-4s\sigma y} - 3p_4 e^{-3s\sigma y}(s\sigma) - \\ & 2p_5 s\sigma e^{-2s\sigma y} + p_6 s\sigma e^{-s\sigma y} + 4s\sigma p_7 e^{s\sigma y} + 3p_8 e^{s\sigma y}(s\sigma) + 2p_9 s\sigma e^{-2s\sigma y} \\ & + p_{10}\left[ys\sigma e^{s\sigma y} + e^{s\sigma y}\right] + p_{11}\left(e^{-2s\sigma y} - 2s\sigma y e^{-2s\sigma y} + e^{-2s\sigma y}\frac{8s\sigma y}{3s\sigma}\right) \\ & - p_{12}\left(e^{-s\sigma y} y - \frac{y^2}{2} e^{-s\sigma y} s\sigma + e^{-2s\sigma y}\frac{1}{2s\sigma} - \frac{y}{2s\sigma} s\sigma y e^{-2s\sigma y}\right) \\ & + p_{13}\left(e^{2s\sigma y} y + 2s\sigma y e^{2s\sigma y} + e^{2s\sigma y}\frac{8s\sigma y}{3s\sigma}\right) \\ & + p_{14}\left(e^{s\sigma y} y + \frac{y^2}{2} s\sigma e^{s\sigma y} - e^{s\sigma y}\frac{1}{2s\sigma} - \frac{y}{2s\sigma} s\sigma e^{s\sigma y}\right) \\ & - 4p_{15} - 3p_{16} y^2 - 2p_{17} y - p_{18}. \end{aligned}$$

The shear stresses at the plates $y = 0$ and $y = 1$ are given by

$$\tau_1=\left(\frac{du}{dy}\right)_{y=o}$$

$$=-p_1 s\sigma+p_2 s\sigma-4p_3 s\sigma-3p_4 s\sigma-2p_5 s\sigma+ p_6 s\sigma+4p_7 s\sigma+3p_8 s\sigma+2p_9 s\sigma+p_{10}+p_{11}- p_{12}\left(\frac{1}{2s\sigma}\right)+p_{13}\left(\frac{11}{3}\right)-p_{14}\left(\frac{1}{2s\sigma}\right)-p_{18}.$$

$$\tau_2=\left(\frac{du}{dy}\right)_{y=1}$$

$$=-s\sigma p_1 e^{-s\sigma}+s\sigma p_2 e^{s\sigma}-4p_3 s\sigma e^{-4s\sigma}-3p_4 s\sigma e^{-3s\sigma} +p_{10}\left[s\sigma\left(1+e^{s\sigma}\right)\right]+p_{11}\left[e^{-2s\sigma}\left(1-2s\sigma+\frac{8}{3}\right)\right] -p_{12}\left[\frac{1}{2}e^{-s\sigma}+\frac{1}{2}e^{-s\sigma}\left(s\sigma+\frac{1}{s\sigma}\right)\right]+p_{13}\left[e^{2s\sigma}\left(1+2s\sigma+\frac{8}{3}\right)\right] +p_{14}\left[\frac{1}{2}e^{s\sigma}\left(1+s\sigma-\frac{1}{s\sigma}\right)\right]-4p_{15}-3p_{16}-2p_{17}-p_{18}$$

3.1.2. Rate of Heat Transfer:

The dimensionless Nusselt number is defined by

$$Nu=\frac{dT}{dy}$$

$$=-4N_1 e^{-4s\sigma y}-3N_2 e^{-3s\sigma y}-2s\sigma e^{-2s\sigma y}\left(N_3+N_{10}\right)-s\sigma e^{-s\sigma y}\left(N_4+N_{12}\right) +4N_5 s\sigma e^{4s\sigma y}+3N_6 s\sigma e^{3s\sigma y}+2s\sigma e^{2s\sigma y}\left(N_7-N_{14}\right)+s\sigma e^{s\sigma y}\left(N_8-N_{16}\right) +N_9\left[e^{-2s\sigma y}-2s\sigma y e^{-2s\sigma y}\right]+N_{11}\left[e^{-s\sigma y}-ys\sigma e^{-s\sigma y}\right]+N_{13}\left[e^{2s\sigma y}+2s\sigma y e^{2s\sigma y}\right] +N_{15}\left[e^{s\sigma y}+s\sigma y e^{s\sigma y}\right]+4N_{17}y^3+3N_{18}y^2+2N_{19}y+M_1.$$

The Nusselt numbers at the plates $y=0$ and $y=1$ are given by

$$Nu_1=\left(\frac{dT}{dy}\right)_{y=0}$$

$$=-4N_1 s\sigma-3N_2 s\sigma-2\left(N_3+N_{10}\right)s\sigma-\left(N_4+N_{12}\right)s\sigma+4N_5 s\sigma+3N_6 s\sigma +2\left(N_7-N_{14}\right)s\sigma+\left(N_8-N_{16}\right)s\sigma+N_9+N_{11}+N_{13}+N_{15}+M_1$$

$$Nu_2=\left(\frac{dT}{dy}\right)_{y=1}$$

$$=-4N_1 s\sigma e^{-4s\sigma}-3N_2 s\sigma e^{-3s\sigma}-2s\sigma e^{-2s\sigma}\left(N_3+N_{10}\right)-s\sigma e^{-s\sigma}\left(N_4+N_{12}\right) +4N_5 s\sigma e^{4s\sigma}+3N_6 s\sigma e^{3s\sigma}+2s\sigma e^{2s\sigma}\left(N_7-N_{14}\right)+s\sigma e^{s\sigma}\left(N_8-N_{16}\right) +N_9\left[e^{-2\sigma}-2s\sigma e^{-2s\sigma}\right]+N_{11}\left[e^{-s\sigma}-s\sigma e^{-s\sigma}\right]+N_{13}\left[e^{2s\sigma}+2s\sigma e^{2s\sigma}\right] +N_{15}\left[e^{s\sigma}+s\sigma e^{s\sigma}\right]+4N_{17}+3N_{18}+2N_{19}+M_1$$

where

$$M_1=1-M_2-N_1 e^{-4s\sigma}-N_2 e^{-3s\sigma}-\left(N_3+N_{10}+N_9\right)e^{-2s\sigma}-\left(N_4+N_{12}+N_{11}\right)e^{-s\sigma} -N_5 e^{4s\sigma}-N_6 e^{3s\sigma}-e^{2s\sigma}\left(N_7-N_{14}+N_{13}\right)-e^{s\sigma}\left(N_8-N_{16}+N_{15}\right)-N_{17}-N_{18}-N_{19}$$

$$M_2=1-N_1-N_2-N_3-N_4-N_5-N_6-N_7-N_8-N_{10}-N_{12}+N_{14}+N_{16}$$

$$P_1=\frac{V\left(1+e^{s\sigma}\right)-Z_1 m_1}{e^{s\sigma}-e^{-s\sigma}},\ N_1=\frac{mc^2}{16s^2\sigma^2};N_2=\frac{mac}{9s^2\sigma^2};$$

$$N_3=\frac{m\left(a^2+2cg\right)}{4s^2\sigma^2};N_4=\frac{m\left(2bc+2ag\right)}{s^2\sigma^2};N_5=\frac{md^2}{16s^2\sigma^2};N_6=\frac{2bd}{9s^2\sigma^2};$$

$$N_7=\frac{m\left(b^2+2dg\right)}{4s^2\sigma^2};N_8=\frac{m\left(2ad+2bg\right)}{s^2\sigma^2};N_9=\frac{mcf}{2s^2\sigma^2};N_{10}=\frac{mcf}{2s^3\sigma^3}$$

$$N_{11}=\frac{2maf}{s^2\sigma^2};N_{12}=\frac{4maf}{s^3\sigma^3};N_{13}=\frac{mdf}{2s^2\sigma^2};N_{14}=\frac{mdf}{s^3\sigma^3};N_{15}=\frac{2mbf}{s^2\sigma^2};$$

$$N_{16}=\frac{2mbf}{s^3\sigma^3};N_{17}=\frac{mf^2}{12};N_{18}=\frac{mfg}{3};N_{19}=\frac{m}{2}\left(2ab+2cd+g^2\right),$$

$$P_2=\frac{V\left(1+e^{-s\sigma}\right)-Z_2 m_1}{\left(e^{-s\sigma}-e^{s\sigma}\right)};P_3=\frac{m_1 N_1}{15s^2\sigma^2};P_4=\frac{m_1 N_2}{8s^2\sigma^2};$$

$$P_5=\frac{m_1\left(N_3+N_{10}\right)}{3s^2\sigma^2};P_6=\frac{m_1\left(N_4+N_{12}\right)}{2s\sigma};P_7=\frac{m_1 N_5}{15s^2\sigma^2};P_8=\frac{m_1 N_6}{8s^2\sigma^2};$$

$$P_9=\frac{m_1\left(N_7-N_{14}\right)}{3s^2\sigma^2};P_{10}=\frac{m_1\left(N_8-N_{10}\right)}{2s\sigma};P_{11}=\frac{m_1 N_9}{3s^2\sigma^2};P_{12}=\frac{m_1 N_{11}}{2s\sigma}$$

$$P_{13}=\frac{m_1 N_{13}}{3s^2\sigma^2};P_{14}=\frac{m_1 N_{15}}{2s\sigma};P_{15}=\frac{m_1 N_{17}}{s^2\sigma^2};P_{16}=\frac{m_1 N_{18}}{s^2\sigma^2};$$

$$P_{17}=m_1\left(\frac{N_{19}}{s^2\sigma^2}+\frac{12N_{17}}{s^4\sigma^4}\right);P_{18}=m_1\left(\frac{M_1}{s^2\sigma^2}+\frac{16N_{18}}{s^4\sigma^4}\right);$$

$$P_{19}=m_1\left(\frac{M_2}{s^2\sigma^2}+\frac{N_{19}}{s^4\sigma^4}+\frac{24N_{17}}{s^6\sigma^6}\right)\ a=F_1\left(-s\sigma\right);b=F_2\left(s\sigma\right);$$

$$c=\frac{-2G_1}{3s\sigma};d=\frac{2G_2}{3s\sigma};f=\frac{-2G_3}{s^2\sigma^2};g=\frac{-G_4}{s^2\sigma^2}.$$

$$Z_1=\begin{Bmatrix}\left(P_3+P_4+P_5+P_7+P_8+P_9-\frac{4P_{11}}{3s\sigma}+\frac{4P_{13}}{3s\sigma}-P_{19}\right)e^{s\sigma}-P_3 e^{-4s\sigma}-P_4 e^{-3s\sigma}-P_5 e^{-2s\sigma}\\ +P_6 e^{-s\sigma}-P_7 e^{4s\sigma}-p_8 e^{3s\sigma}-P_9 e^{2s\sigma}-P_{10}e^{s\sigma}-P_{11}e^{-2s\sigma}\left(1-\frac{4}{3s\sigma}\right)+P_{12}e^{-2s\sigma}\left(\frac{1}{2}+\frac{1}{2s\sigma}\right)\\ -P_{13}e^{2s\sigma}\left(1+\frac{4}{3s\sigma}\right)-P_{14}e^{s\sigma}\left(\frac{1}{2}-\frac{1}{2s\sigma}\right)+P_{15}+P_{16}+P_{17}+P_{18}+P_{19}\end{Bmatrix}$$

$$Z_2=\begin{Bmatrix}\left(P_3+P_4+P_5+P_7+P_8+P_9-\frac{4P_{11}}{3s\sigma}+\frac{4P_{13}}{3s\sigma}-P_{19}\right)e^{-s\sigma}-P_3 e^{-4s\sigma}-P_4 e^{-3s\sigma}-P_5 e^{-2s\sigma}\\ +P_6 e^{-s\sigma}-P_7 e^{4s\sigma}-p_8 e^{3s\sigma}-P_9 e^{2s\sigma}-P_{10}e^{s\sigma}-P_{11}e^{-2s\sigma}\left(1-\frac{4}{3s\sigma}\right)+P_{12}e^{-s\sigma}\left(\frac{1}{2}+\frac{1}{2s\sigma}\right)\\ -P_{13}e^{s\sigma}\left(1+\frac{4}{3s\sigma}\right)-P_{14}e^{s\sigma}\left(\frac{1}{2}-\frac{1}{2s\sigma}\right)+P_{15}+P_{16}+P_{17}+P_{18}+P_{19}\end{Bmatrix}$$

3.2. Shooting Procedure:

$$\frac{d^2u}{dy^2}+\left(1+\lambda_1\right)G\theta-\sigma^2 u=0 \tag{9}$$

$$\frac{d^2\theta}{dy^2}+\frac{PE}{\left(1+\lambda_1\right)}\left(\frac{du}{dy}\right)^2=0 \tag{10}$$

$$u=V,\ \theta=1\ \ at\ \ y=0$$
$$u=-V,\ \theta=1\ at\ \ y=1 \tag{11}$$

The interval of solution [0,1] is divided into N equal subintervals of constant step length h. Let $0=y_0,y_1,...,y_N=1$ be the mesh points.

Then we have $y_i=ih$, $i=0,1,...,N$

The initial slopes $\frac{du}{dy}=\alpha$ (say), $\frac{d\theta}{dy}=\beta$ (say) are assumed appropriately, and hence the set of initial value problems is formulated as

$$\frac{d^2u}{dy^2}+\left(1+\lambda_1\right)G\theta-\sigma^2 u=0 \tag{21}$$

$$\frac{d^2\theta}{dy^2}+\frac{PE}{\left(1+\lambda_1\right)}\left(\frac{du}{dy}\right)^2=0 \tag{22}$$

$$u(y=0)=V,\left.\frac{du}{dy}\right|_{y=0}=\alpha \tag{23}$$

$$\theta(y=0)=1,\left.\frac{d\theta}{dy}\right|_{y=0}=\beta \tag{24}$$

This system of equations is solved by shooting method. We used Runge – Kutta method of order four with initial guesses α , β for the unknown slopes $\frac{du}{dy}$, $\frac{d\theta}{dy}$ .The values of these conditions are then iteratively obtained through Newton's method such that solutions satisfy the conditions $u=-V;\theta=1$ at the other boundary $y=1$ with error less than 10^{-5} .

4. Numerical Results:

Numerical results have been obtained by both the procedures described in sections 3.1 and 3.2. It is noted that by both the methods, the results are in good agreement. Hence, the methods proposed here will be a good approximation for the solution of the non–linear boundary value problem (9)-(10). Here, we furnish the results for velocity distribution, temperature distribution, skin friction and rate of heat transfer effects on flow by the method proposed in section 3.1. Also the results for velocity and temperature distribution by the method proposed in section 3.2 are presented and compared.

For the different values of physical parameters G, E, V, λ_1 and σ considered in Table 1, the numerical values of velocity and temperature distribution for $P=0.71$ by Iteration procedure are presented in Tables 2 and 3 respectively. The corresponding graphs for velocity and temperature distributions for $P=0.71$ are shown in figures 2 and 3 respectively.

For the various values of physical parameters G, E, P, V, λ_1 and σ considered in Table 4, the numerical values of velocity and temperature distribution for different values of P by Iteration procedure are given in Tables 5 and 6 respectively. The corresponding graphs for velocity and temperature distributions for different values of P are shown in figures 4 and 5 respectively.

For the different values of physical parameters G, E, V, λ_1 and σ considered in Table 7, the numerical values of velocity and temperature distribution for $P=0.71$ by shooting method are presented in Tables 8 and 9 respectively. The corresponding graphs for velocity and temperature distributions for $P=0.71$ are shown in figures 6 and 7 respectively.

For the various values of physical parameters G, E, P, V, λ_1 and σ considered in Table 10, the numerical values of velocity and temperature distribution for various values of P by shooting method are given in Tables 11 and 12 respectively. The corresponding graphs for velocity and temperature distributions for various values of P are presented in figures 8 and 9 respectively.

For different values of physical parameters G, E, λ_1 and σ considered in Table 13, the numerical values for skin friction at the plates $y=0$ and $y=1$ for $P=0.71$ and $P=7$ by Iteration procedure are given in Tables 14 and 15 respectively The corresponding graphs are presented in figures 10 and 11 respectively.

For different values of physical parameters G, E, λ_1 and σ considered in Table 13, the numerical values of Rate of heat transfer coefficient at the plates $y=0$ and $y=1$ for $P=0.71$ and $P=7$ by Iteration procedure given in Tables 16 and 17 respectively. The corresponding graphs are in figures 12 and 13 respectively.

The velocity u_3 and the temperature θ_3 have also been calculated and they being very large terms are not presented here for the sake of conciseness. Giving several sets of values to the non-dimensional parameters G, E, P, V, λ_1 and σ the non-dimensional velocities u_2, u_3 and non-dimensional temperatures θ_2, θ_3 have been calculated numerically. It has been found that u_2, u_3 and θ_2, θ_3 do not differ significantly hence, we consider u_3 as u and θ_3 as θ.

5. Discussion:

As mentioned earlier, the numerical solution for the velocity u , the temperature θ. are expected to explain the flow in the porous medium with heat transfer characteristics of the fluid in the belt everywhere, except perhaps, at the two ends as shown in figure 1. Fluids having with high viscosity will have small Grashof number G . The smallness of the Grashof number G may be due to smallness of the temperature differences.

Figure 2, shows that the behaviour of flow of air at $P=0.71$ for various values of G, E, V, λ_1 and σ by Iteration procedure. We observed that an increase in the Grashof number G effects the enhancement in fluid velocity. The higher values of Eckert number E effects comparatively small enhancement in the fluid velocity. An increase of the porous material σ reduces the fluid velocity. Similarly an increase of the Jeffery parameter λ_1 yields the enhancement in the fluid velocity. The plate velocity V increases the fluid velocity near the plate $y=0$ and reduces near the other plate $y=1$. All the behaviour mentioned above in the case of air is true in the case of fluids with high Prandtl numbers as illustrated in figure 4. By using shooting method we observed the same behaviour from the figures 6 and 8.

The temperature of air at $P=0.71$ on G, E, V, λ_1 and σ by Iteration procedure is represented in figure 3. The temperatures of air in the case when the plates are moving are greater than those when the plates are at rest. The increase in the temperature becomes very important when the plates start moving faster. We notice that as G and E takes higher values the fluid temperature enhances. The fluid temperature increases with variation in Prandtl number as given in figure 5. Also, the temperature decreases with an increase of σ and the temperature reduces with an increase in Jeffrey parameter λ_1 .The similar behavior is observed by using shooting method and respective graphs are presented in figures 7 and 9.

Using Iteration procedure it is observed from the figures 10 and 11, the velocity increases at both the plates when the skin friction decreases at both the plates, while it enhances with the increase in any of the other parameters G, E, σ, λ_1 and P. The skin friction is positive at the upward moving plate and negative at the other plate.

Using Iteration method the change in the rate of heat transfer coefficient at both the plates for the various values of λ_1, σ, G and E in the case of air and water at 20^0C are presented in the Figures12and 13 respectively. The rate of heat transfer coefficient is positive at the upward moving plate and negative at the other. That is the heat flow at either plate is from the fluid present in the porous medium. The influence of E, λ_1 and σ is to reduce the heat transfer coefficient at the upward moving plate and to reduce at the other, while the influence of G is to decrease the rate of heat transfer coefficient at both the plates.

We observed that the differential equations (9) – (10) subject to boundary conditions (11) have also been integrated numerically by the well-known Runge – Kutta method and results obtained by Iteration procedure have been observed to be in good agreement with those obtained by the Runge – Kutta method.

6. Conclusions:

In this study, the important observations are summarized as follows.

1. Fluid velocity increases with the parameters G, E, V and P and Jeffrey parameter λ_1 causes increase in fluid velocity.
2. Fluid temperature increases with the parameters G and E and decreases with increase of Jeffrey parameter λ_1 .

3. The skin friction near both plates reduces as the plate velocity increases and enhances with the increase in parameters G, E, λ_1, σ and P.
4. The rate of heat transfer coefficient at the upward moving plate is positive and the other negative.

References:

[1] Ostrach, S., Tech. Notes, Natn. Advis. Comm. Aeronaut., Wash., 2863, (1952).

[2] F.J.Suriano, K.T. Yang and J.A. Donlon. "Laminar free convection along a vertical plate at extremely small Grashof numbers". *International Journal of Heat and Mass Transfer*, Vol. 8, (1965), pp.815-831.

[3] https://doi.org/10.1016/0017-9310 (65)90026-8.

[4] K. Yamamoto and Z. Yoshida. "Flow through a porous wall with convective acceleration". *J. phys. Soct. Japan*, Vol. 37(3) (1974), pp.774-779. https://doi.org/10.1143/JPSJ.37.774.

[5] K. Vajravelu. "Free convection heat transfer between two long, vertical, thin plates moving in opposite directions". *Indian Journal of Technology*, Vol. 16 (1978), pp.399-403.

[6] S. Sreenadh and P.V.Arunachalam. "A model for the study of flow between two permeable beds", *Proceedings of the national symposium on Mathematical modelling*. Mehta Research Institute, Allahabad, (1982).

[7] K.R. Rajagopal, A.S. Gupta. "An exact solution for the flow of a non-Newtonian fluid past an infinite porous plate". *Meccanica*, Vol. 19(2) (1984), pp.158–160. https://doi.org/10.1007/BF01560464.

[8] K. Vajravelu, S. Sreenadh and P. Lakshminaryana. "The influence of heat transfer on peristaltic transport of a Jeffrey fluid in a vertical porous stratum", *Communications in Nonlinear Science and Numerical Simulation*, Vol. 16 (8) (2011), pp. 3107-3125. https://doi.org/10.1016/j.cnsns.2010.11.001.

[9] J.C. Umavathi and M. Shekar. "Unsteady mixed convective flow and heat transfer in a vertical corrugated channel with composite porous media". *Journal of Engineering Physics and Thermophysics*, Vol. 86(4) (2013), pp.754 – 765. https://doi.org/10.1007/s10891-013-0892-1.

[10] A. Raptis and Kafousias. "Heat transfer in flow through a porous medium bounded by an infinite vertical plate under the action of a magnetic field". *Int. J. Energy Res.*, Vol. 6(3) (1982), pp.241-245. https://doi.org/10.1002/er.4440060305.

[11] A.N.S.Srinvias, S.Sreenadh, B.Govindarajulu and R.H.Reddy. "Free flow of a Jeffrey fluid between two long vertical thin plates". *International Journal of Pure and Applied Mathematics*, Vol. 103 (4) (2015), pp. 635-652. http://dx.doi.org/10.12732/ijpam.v103i4.4.

Table 1: Values of various physical parameters

Profile	G	E	V	λ_1	σ
I	0.2	0.01	0.0	0.1	1
II	0.2	0.01	0.5	0.1	1
III	0.2	0.01	2.0	0.1	1
IV	0.8	0.01	0.5	0.1	1
V	0.8	0.01	2.0	0.1	1
VI	0.8	0.02	0.5	0.1	1
VII	0.8	0.02	2.0	0.1	1
VIII	0.8	0.02	0.5	0.2	1
IX	0.8	0.02	2.0	0.2	1
X	0.8	0.02	0.5	0.1	2
XI	0.8	0.02	2.0	0.1	2

Table 2: Velocity distribution for P=0.71

y	I	II	III	IV	V	VI	VII	VIII	IX	X	XI
0.0	0.00000	0.50000	2.00000	0.50000	2.00000	0.50000	2.00000	0.50000	2.00000	0.50000	2.00000
0.1	0.00908	0.40321	1.58566	0.43047	1.61315	0.43049	1.61347	0.43380	1.61677	0.40720	1.54119
0.2	0.01605	0.30826	1.18498	0.35645	1.23359	0.35648	1.23420	0.36232	1.24004	0.32191	1.13534
0.3	0.02098	0.21418	0.79394	0.27718	0.85752	0.27723	0.85835	0.28486	0.86598	0.24070	0.76610
0.4	0.02392	0.12005	0.40862	0.19187	0.48112	0.19193	0.48211	0.20063	0.49081	0.16031	0.41861
0.5	0.02490	0.02491	0.02516	0.09967	0.10064	0.09973	0.10167	0.10879	0.11073	0.07752	0.07891
0.6	0.02392	-0.07218	-0.36027	-0.00035	-0.28776	-0.00029	-0.28676	0.00841	-0.27806	-0.01100	-0.26666
0.7	0.02098	-0.17219	-0.75154	-0.10919	-0.68795	-0.10913	-0.68709	-0.10150	-0.67946	-0.10881	-0.63194
0.8	0.01605	-0.27613	-1.15256	-0.22793	-1.10392	-0.22789	-1.10329	-0.22205	-1.09745	-0.21983	-1.03159
0.9	0.00908	-0.38504	-1.56733	-0.35777	-1.53983	-0.35775	-1.53949	-0.35445	-1.53619	-0.34851	-1.48160
1.0	0.00000	-0.50001	-2.00000	-0.50000	-2.00000	-0.50000	-1.99999	-0.50000	-1.99999	-0.50000	-1.99999

Table 3: Temperature distribution for P=0.71

y	I	II	III	IV	V	VI	VII	VIII	IX	X	XI
0.0	1.00000	1.00000	1.00000	1.00000	1.00000	1.00000	1.00000	1.00000	1.00000	1.00000	1.00000
0.1	1.00000	1.00027	1.00452	1.00023	1.00434	1.00047	1.00867	1.00042	1.00791	1.00047	1.00853
0.2	1.00000	1.00048	1.00798	1.00044	1.00773	1.00087	1.01545	1.00079	1.01411	1.00083	1.01463
0.3	1.00000	1.00064	1.01041	1.00060	1.01020	1.00120	1.02039	1.00109	1.01865	1.00111	1.01878
0.4	1.00000	1.00073	1.01188	1.00072	1.01176	1.00144	1.02351	1.00132	1.02153	1.00130	1.02127
0.5	1.00000	1.00077	1.01239	1.00079	1.01239	1.00158	1.02478	1.00145	1.02272	1.00141	1.02224
0.6	1.00000	1.00075	1.01195	1.00080	1.01208	1.00160	1.02416	1.00148	1.02217	1.00142	1.02171
0.7	1.00000	1.00067	1.01054	1.00074	1.01076	1.00148	1.02153	1.00138	1.01979	1.00132	1.01957
0.8	1.00000	1.00052	1.00813	1.00060	1.00838	1.00120	1.01677	1.00112	1.01543	1.00109	1.01557
0.9	1.00000	1.00030	1.00464	1.00036	1.00483	1.00072	1.00967	1.00067	1.00891	1.00067	1.00927
1.0	1.00000	1.00000	1.00000	1.00000	1.00000	1.00000	1.00000	1.00000	1.00000	1.00000	1.00000

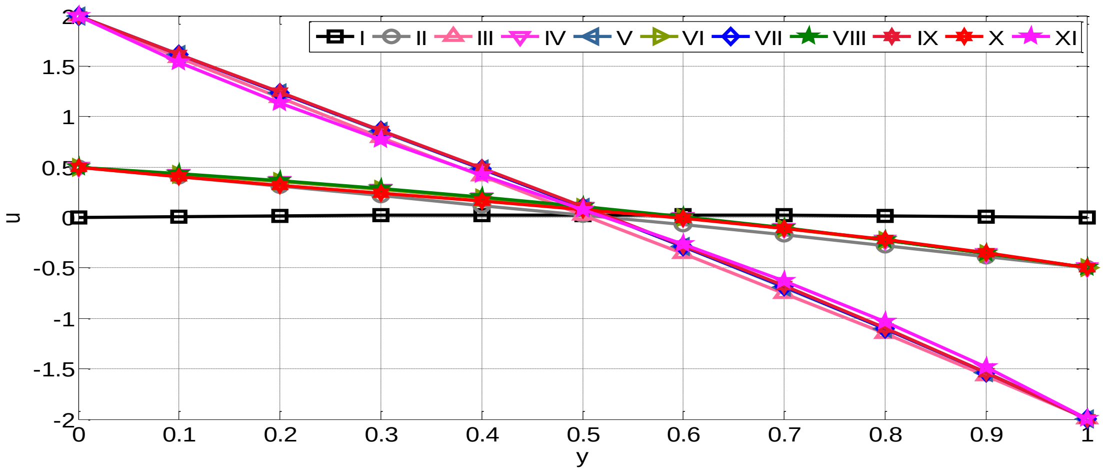

Fig 2: Velocity distribution for P=0.71.

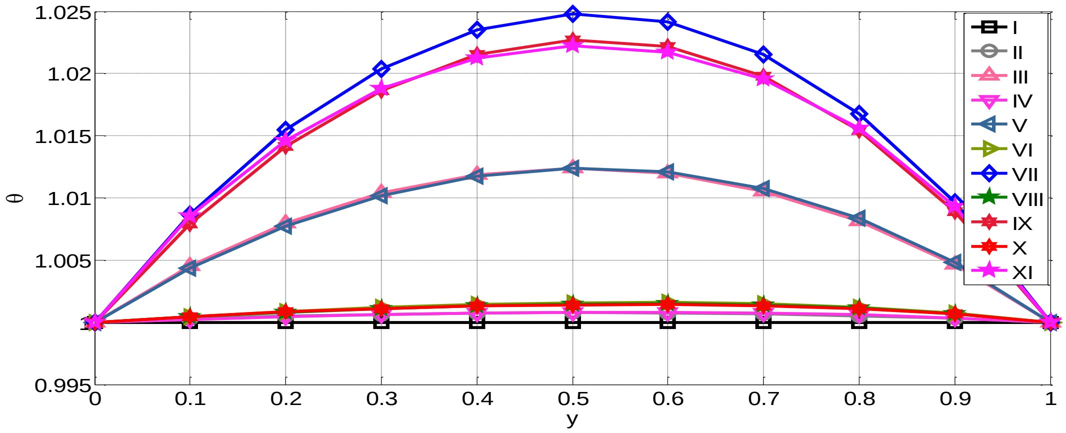

Fig 3: Temperature distribution for P=0.71.

Table 4: Values of various physical parameters.

Profile	G	E	P	V	λ_1	σ
I	0.5	0.01	3	0.0	0.1	1
II	0.5	0.01	3	2.0	0.1	1
III	0.5	0.01	7	0.5	0.1	1
IV	0.5	0.01	7	2.0	0.1	1
V	0.5	0.02	7	0.5	0.1	1
VI	0.5	0.02	7	2.0	0.1	1
VII	0.8	0.01	7	0.5	0.1	1
VIII	0.8	0.01	7	2.0	0.1	1
IX	0.8	0.01	7	0.5	0.2	1
X	0.8	0.01	7	2.0	0.2	1
XI	0.8	0.01	7	0.5	0.1	2
XII	0.8	0.01	7	2.0	0.1	2

Table 5: Velocity distribution for various values of P.

y	I	II	III	IV	V	VI	VII	VIII	IX	X	XI	XII
0.0	0.00000	2.00000	0.50000	2.00000	0.50000	2.00000	0.50000	2.00000	0.50000	2.00000	0.50000	2.00000
0.1	0.02271	1.60005	0.41695	1.60118	0.41707	1.60316	0.43065	1.61598	0.43395	1.61927	0.40731	1.54301
0.2	0.04014	1.21051	0.33256	1.21266	0.33279	1.21640	0.35678	1.23896	0.36262	1.24480	0.32212	1.13877
0.3	0.05246	0.82741	0.24597	0.83035	0.24629	0.83550	0.27764	0.86490	0.28527	0.87252	0.24099	0.77079
0.4	0.05981	0.44685	0.15630	0.45031	0.15668	0.45636	0.19242	0.48981	0.20112	0.49851	0.16066	0.42411
0.5	0.06225	0.06498	0.06265	0.06863	0.06306	0.07501	0.10025	0.10981	0.10931	0.11887	0.07789	0.08470
0.6	0.05981	-0.32202	-0.03592	-0.31853	0.03553	-0.31242	0.00022	-0.27896	0.00892	-0.27026	-0.01064	-0.26109
0.7	0.05246	-0.71803	-0.14039	-0.71504	-0.14005	-0.70979	-0.10869	-0.68038	-0.10106	-0.67275	-0.10850	-0.62714
0.8	0.04014	-1.12699	-0.25181	-1.12478	-0.25156	-1.12093	-0.22756	-1.09836	-0.22172	-1.09251	-0.21959	-1.02804
0.9	0.02271	-1.55291	-0.37128	-1.55174	-0.37115	-1.54969	-0.35757	-1.53687	-0.35426	-1.53356	-0.34837	-1.47970
1.0	0.00000	-2.00000	-0.50000	-2.00000	-0.49999	-2.00000	-0.49999	-2.00000	-0.49999	-2.00000	-0.49999	-2.00000

Table 6: Temperature distribution for various values of P.

y	I	II	III	IV	V	VI	VII	VIII	IX	X	XI	XII
0.0	1.00000	1.00000	1.00000	1.00000	1.00000	1.00000	1.00000	1.00000	1.00000	1.00000	1.00000	1.00000
0.1	1.00002	1.01870	1.00247	1.04353	1.00494	1.08676	1.00231	1.04256	1.00208	1.03882	1.00230	1.04190
0.2	1.00003	1.03314	1.00450	1.07720	1.00900	1.15397	1.00429	1.07591	1.00389	1.06933	1.00410	1.07191

0.3	1.00003	1.04351	1.00607	1.10141	1.01213	1.20243	1.00591	1.10029	1.00539	1.09172	1.00546	1.09239
0.4	1.00004	1.04991	1.00714	1.11638	1.01428	1.23253	1.00709	1.11576	1.00650	1.10600	1.00640	1.10474
0.5	1.00004	1.05235	1.00768	1.12214	1.01536	1.24427	1.00779	1.12218	1.00717	1.11202	1.00693	1.10963
0.6	1.00004	1.05077	1.00764	1.11853	1.01528	1.23727	1.00789	1.11924	1.00730	1.10946	1.00700	1.10712
0.7	1.00003	1.04503	1.00694	1.10519	1.01390	1.21075	1.00732	1.10641	1.00679	1.09780	1.00652	1.09664
0.8	1.00003	1.03489	1.00551	1.08155	1.01104	1.16353	1.00592	1.08296	1.00552	1.07634	1.00536	1.07693
0.9	1.00002	1.02003	1.00324	1.04683	1.00650	1.09399	1.00354	1.04791	1.00332	1.04414	1.00329	1.04585
1.0	1.00000	1.00000	1.00000	1.00000	1.00000	1.00000	1.00000	1.00000	1.00000	1.00000	1.00000	0.99999

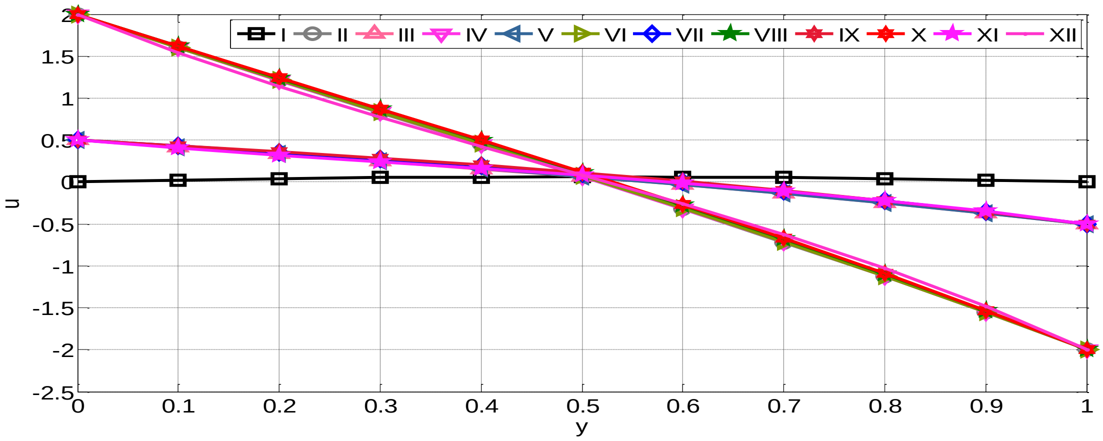

Fig 4: Velocity distribution for various values of P

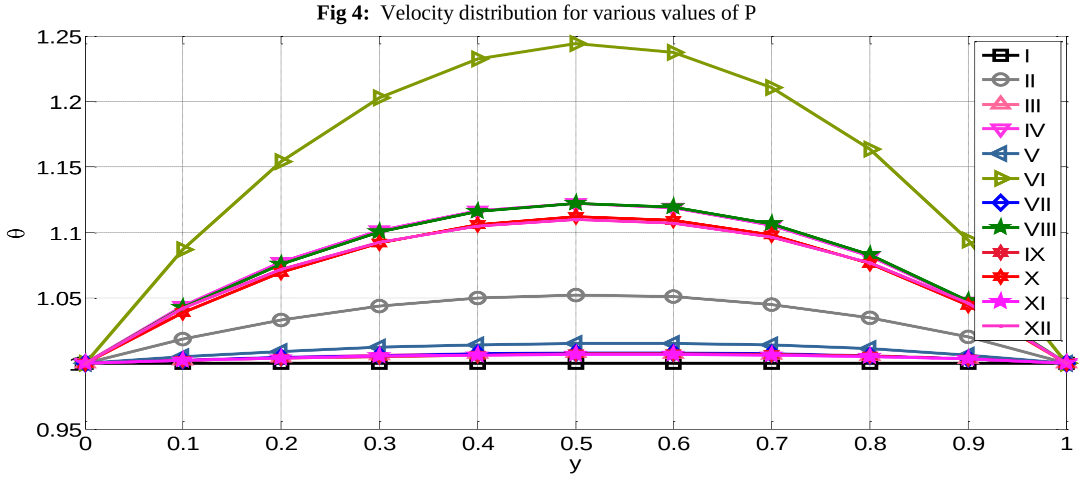

Fig 5: Temperature distribution for various values of P

Table 7: Values of various physical parameters.

Profile	G	E	V	λ_1	σ
I	0.2	0.01	0.0	0.1	1
II	0.2	0.01	1.0	0.1	1
III	0.2	0.01	2.0	0.1	1
IV	0.8	0.01	1.0	0.1	1
V	0.8	0.01	2.0	0.1	1
VI	0.8	0.02	1.0	0.1	1
VII	0.8	0.02	2.0	0.1	1
VIII	0.8	0.02	1.0	0.2	1
IX	0.8	0.02	2.0	0.2	1
X	0.8	0.02	1.0	0.1	2
XI	0.8	0.02	2.0	0.1	2

Table 8: Velocity distribution for P=0.71

y	I	II	III	IV	V	VI	VII	VIII	IX	X	XI
0.0	0.00000	1.00000	2.00000	1.00000	2.00000	1.00000	2.00000	1.00000	2.00000	1.00000	2.00000
0.1	0.00908	0.79735	1.58566	0.82466	1.61315	0.82474	1.61347	0.82804	1.61677	0.78514	1.54119
0.2	0.01605	0.60048	1.18498	0.64875	1.23359	0.64890	1.23420	0.65474	1.24004	0.59294	1.13534
0.3	0.02098	0.40741	0.79394	0.47052	0.85752	0.47073	0.85835	0.47836	0.86598	0.41568	0.76610
0.4	0.02392	0.21621	0.40862	0.28816	0.48112	0.28841	0.48211	0.29711	0.49081	0.24624	0.41861
0.5	0.02490	0.02496	0.02516	0.09986	0.10064	0.10012	0.10167	0.10918	0.11073	0.07780	0.07891
0.6	0.02392	-0.16824	-0.36027	-0.09628	-0.28776	-0.09603	-0.28676	-0.08733	-0.27806	-0.09640	-0.26666
0.7	0.02098	-0.36533	-0.75154	-0.30222	-0.68795	-0.30200	-0.68709	-0.29436	-0.67946	-0.28334	-0.63194
0.8	0.01605	-0.56829	-1.15256	-0.52001	-1.10392	-0.51984	-1.10329	-0.51401	-1.09745	-0.49052	-1.03159
0.9	0.00908	-0.77914	-1.56733	-0.75183	-1.53983	-0.75174	-1.53949	-0.74844	-1.53619	-0.72626	-1.48160
1.0	0.00000	-1.00000	-2.00000	-1.00000	-2.00000	-0.99999	-1.99999	-0.99999	-1.99999	-1.00000	-1.99999

Table 9: Temperature distribution for P=0.71.

y	I	II	III	IV	V	VI	VII	VIII	IX	X	XI
0.0	1.00000	1.00000	1.00000	1.00000	1.00000	1.00000	1.00000	1.00000	1.00000	1.00000	1.00000
0.1	1.00000	1.00112	1.00452	1.00103	1.00434	1.00206	1.00867	1.00187	1.00791	1.00204	1.00853
0.2	1.00000	1.00197	1.00798	1.00186	1.00773	1.00372	1.01545	1.00339	1.01411	1.00354	1.01463
0.3	1.00000	1.00259	1.01041	1.00249	1.01020	1.00498	1.02039	1.00455	1.01865	1.00459	1.01878
0.4	1.00000	1.00296	1.01188	1.00291	1.01176	1.00582	1.02351	1.00533	1.02153	1.00526	1.02127
0.5	1.00000	1.00310	1.01239	1.00311	1.01239	1.00622	1.02478	1.00571	1.02272	1.00557	1.02224
0.6	1.00000	1.00300	1.01195	1.00307	1.01208	1.00614	1.02416	1.00565	1.02217	1.00550	1.02171
0.7	1.00000	1.00265	1.01054	1.00277	1.01076	1.00555	1.02153	1.00512	1.01979	1.00501	1.01957
0.8	1.00000	1.00205	1.00813	1.00219	1.00838	1.00438	1.01677	1.00405	1.01543	1.00403	1.01557
0.9	1.00000	1.00118	1.00464	1.00128	1.00483	1.00256	1.00967	1.00238	1.00891	1.00243	1.00927
1.0	1.00000	1.00000	1.00000	1.00000	1.00000	1.00001	1.00000	1.00001	1.00000	1.00000	1.00000

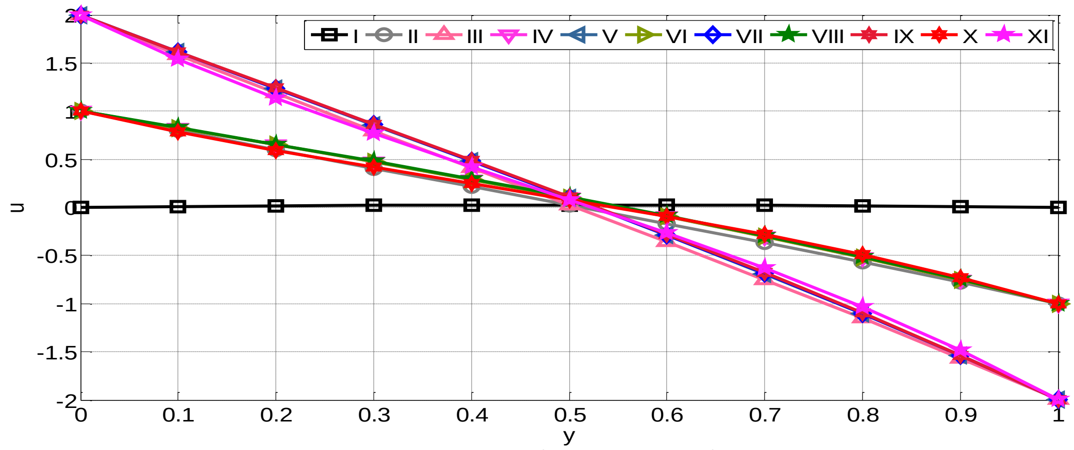

Fig 6: Velocity distribution for various values of P=0.71

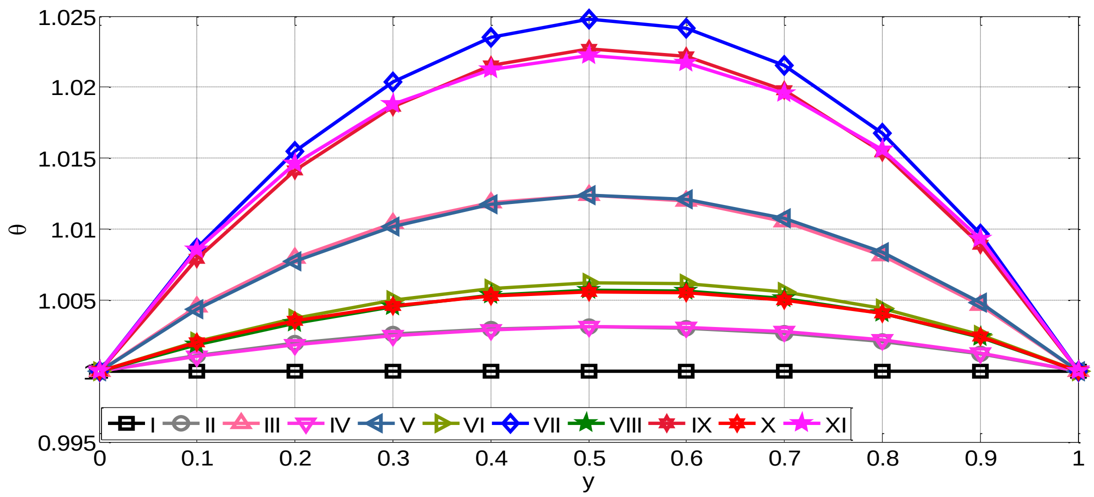

Fig 7: Temperature distribution for various values of P=0.71.

Table 10: Values of various physical parameters.

Profile	G	E	P	V	λ_1	σ
I	0.5	0.01	3	0.0	0.1	1
II	0.5	0.01	3	2.0	0.1	1
III	0.5	0.01	7	1.0	0.1	1
IV	0.5	0.01	7	2.0	0.1	1
V	0.5	0.02	7	1.0	0.1	1
VI	0.5	0.01	7	2.0	0.1	1
VII	0.8	0.01	7	1.0	0.1	1
VIII	0.8	0.02	7	2.0	0.1	1
IX	0.8	0.01	7	1.0	0.2	1
X	0.8	0.01	7	2.0	0.2	1
XI	0.8	0.01	7	1.0	1.0	2

Table 11: Velocity distribution for various values of P.

y	I	II	III	IV	V	VI	VII	VIII	IX	X	XI
0.0	0.00000	2.00000	1.00000	2.00000	1.00000	2.00000	1.00000	2.00000	1.00000	2.00000	1.00000
0.1	0.02271	1.60005	0.81145	1.60118	0.81194	1.60118	0.82536	1.61911	0.82866	1.61927	0.80957
0.2	0.04014	1.21051	0.62545	1.21266	0.62639	1.21266	0.65009	1.24493	0.65592	1.24480	0.63550

0.3	0.05246	0.82741	0.44012	0.83035	0.44140	0.83035	0.47236	0.87310	0.47999	0.87252	0.47073
0.4	0.05981	0.44685	0.25355	0.45031	0.25505	0.45031	0.29033	0.49947	0.29903	0.49851	0.30862
0.5	0.06225	0.06498	0.06385	0.06863	0.06544	0.06863	0.10216	0.12003	0.11122	0.11887	0.14262
0.6	0.05981	-0.32202	-0.13088	-0.31853	-0.12935	-0.31853	-0.09407	-0.26916	-0.08536	-0.27026	-0.03396
0.7	0.05246	-0.71803	-0.33258	-0.71504	-0.33127	-0.71504	-0.30031	-0.67195	-0.29267	-0.67275	-0.22820
0.8	0.04014	-1.12699	-0.54327	-1.12478	-0.54231	-1.12478	-0.51860	-1.09215	-0.51276	-1.09251	-0.44788
0.9	0.02271	-1.55291	-0.76502	-1.55174	-0.76451	-1.55174	-0.75108	-1.53357	-0.74778	-1.53356	-0.70177
1.0	0.00000	-2.00000	-0.99999	-2.00000	-1.00000	-2.00000	-1.00000	-2.00000	-1.00000	-2.00000	-0.99999

Table 12; Temperature distribution for various values of *P*.

y	I	II	III	IV	V	VI	VII	VIII	IX	X	XI
0.0	1.00000	1.00000	1.00000	1.00000	1.00000	1.00000	1.00000	1.00000	1.00000	1.00000	1.00000
0.1	1.00002	1.01870	1.01054	1.04353	1.02104	1.04353	1.01012	1.08465	1.00919	1.03882	1.00514
0.2	1.00003	1.03314	1.01884	1.07720	1.03764	1.07720	1.01830	1.15116	1.01667	1.06933	1.00911
0.3	1.00003	1.04351	1.02496	1.10141	1.04988	1.10141	1.02451	1.19999	1.02237	1.09172	1.01207
0.4	1.00004	1.04991	1.02888	1.11638	1.05774	1.11638	1.02866	1.23118	1.02623	1.10600	1.01411
0.5	1.00004	1.05235	1.03056	1.12214	1.06112	1.12214	1.03064	1.24437	1.02811	1.11202	1.01521
0.6	1.00004	1.05077	1.02989	1.11853	1.05982	1.11853	1.03028	1.23885	1.02785	1.10946	1.01529
0.7	1.00003	1.04503	1.02674	1.10519	1.05353	1.10519	1.02737	1.21347	1.02523	1.09780	1.01419
0.8	1.00003	1.03489	1.02089	1.08155	1.04185	1.08155	1.02160	1.16665	1.01996	1.07634	1.01162
0.9	1.00002	1.02003	1.01209	1.04683	1.02424	1.04683	1.01263	1.09635	1.01170	1.04414	1.00712
1.0	1.00000	1.00000	.99999	1.00000	1.00000	1.00000	1.00000	.99999	1.00000	1.00000	1.00000

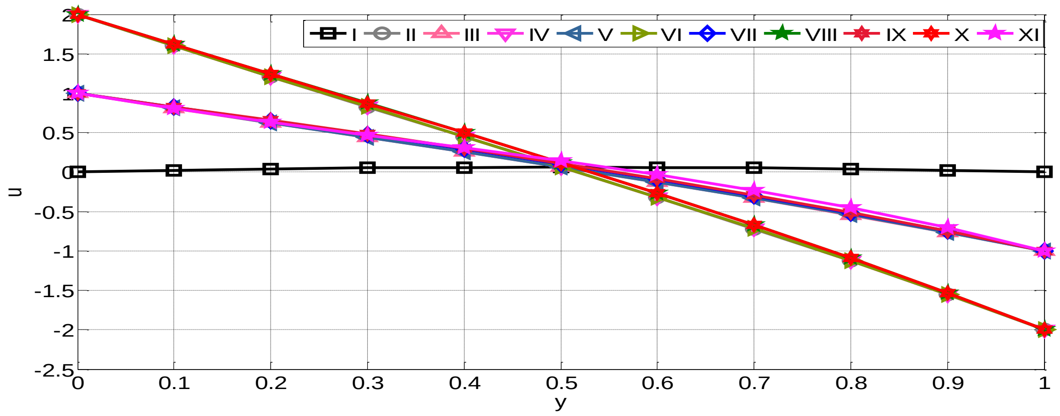

Fig 8: Velocity distribution for various values of P.

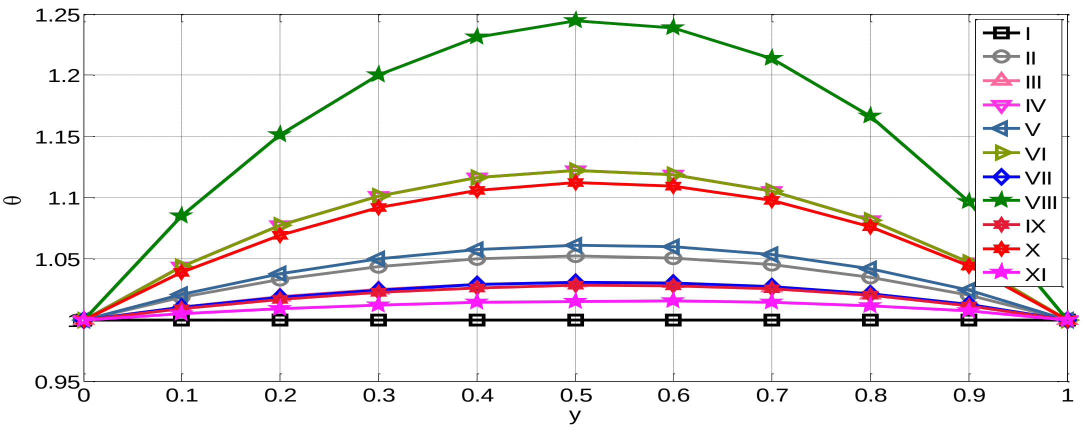

Fig 9: Temperature distribution for various values of P.

Table 13: Values of various physical parameters

Profile	G	E	λ1	σ
I	0.2	0.01	0.1	2
II	0.5	0.01	0.1	2
III	0.5	0.01	0.1	2
IV	0.8	0.02	0.1	2
V	0.2	0.02	0.2	2
VI	0.2	0.01	0.1	3
VII	0.2	0.01	0.1	2
VIII	0.5	0.01	0.1	2
IX	0.5	0.01	0.1	2
X	0.8	0.02	0.1	2
XI	0.2	0.02	0.2	2
XII	0.2	0.01	0.1	3

Table 14: Skin friction at the plates *y*=0 and *y*=1: *P*=0.71.

v	I	II	III	IV	V	VI	VII	VIII	IX	X	XI	XII
0	0.0082	0.20443	0.20451	0.32692	0.08739	0.06405	-0.0816	-0.2038	-0.204	-0.3257	-0.08721	-0.06384
0.2	-0.4550	-0.0332	-0.0332	-0.0209	-0.0461	-0.0622	-0.0619	-0.74182	-0.74185	-0.8648	-0.0636	-0.0750
0.4	-0.0992	-0.0869	-0.0869	-0.0746	-1.01	-1.31	-1.15585	-1.27886	-1.27898	-1.4019	-1.18457	-1.43588
0.6	-1.52874	-1.40566	-1.40543	-1.28258	-1.55792	-1.99332	-1.69284	-1.81595	-1.81624	-1.9391	-1.73314	-2.12176
0.8	-2.06559	-1.94239	-1.94199	-1.81917	-2.10635	-2.67911	-2.22985	-2.35312	-2.35361	-2.4765	-2.28172	-2.80767
1	-2.60242	-2.47905	-2.47846	-2.35567	-2.65477	-3.36489	-2.76688	-2.89037	-2.89111	-3.0139	-2.83034	-3.49361
1.2	-3.13923	-3.01566	-3.01486	-2.8921	-3.20316	-4.05066	-3.30394	-3.42769	-3.42872	-3.5516	-3.37897	-4.17957
1.4	-3.67601	-3.55222	-3.55122	-3.42848	-3.75153	-4.7364	-3.84103	-3.96509	-3.96643	-4.0893	-3.92764	-4.86557
1.6	-4.21277	-4.08872	-4.08757	-3.96484	-4.29988	-5.42213	-4.37815	-4.50258	-4.50423	-4.6272	-4.47633	-5.55161
1.8	-4.74951	-4.62518	-4.62395	-4.50121	-4.84821	-6.10784	-4.91529	-5.04014	-5.04208	-5.1651	-5.02505	-6.23768
2	-5.28623	-5.1616	-5.16041	-5.03764	-5.39651	-6.79353	-5.45246	-5.57778	-5.57995	-5.7031	-5.5738	-6.9238

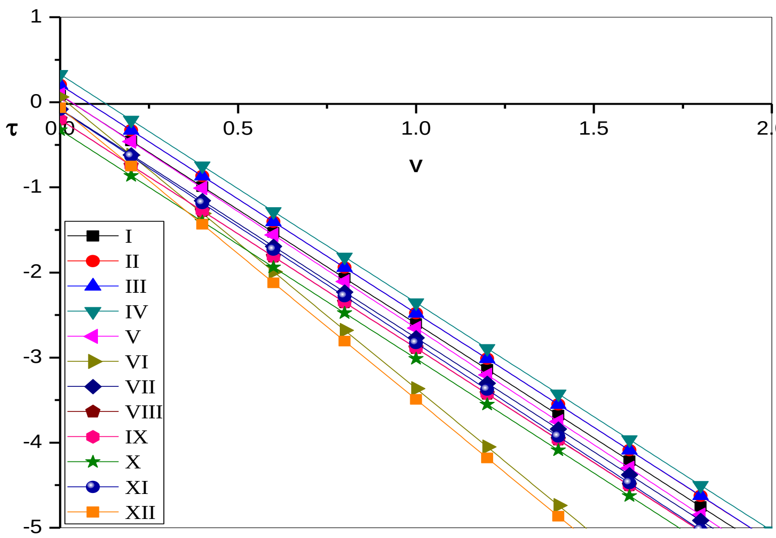

Fig.10: Skin friction at the plates y=0 and *y*=1: *P*=0.71.

Table 15: Skin friction at the plates *y*=0 and *y*=1: *P*=7.

v	I	II	III	IV	V	VI	VII	VIII	IX	X	XI	XII
0	0.0820	0.20321	0.20142	0.25448	0.08198	0.06374	-0.08028	-0.20084	-0.19651	-0.1494	-0.07382	-0.06294
0.2	-0.04550	-0.332	-0.332	-0.209	-0.461	-0.622	-0.619	-0.74204	-0.74226	-0.865	-0.636	-0.750
0.4	-0.092	-0.868	-0.868	-0.745	-1.01	-1.31	-1.15628	-1.27984	-1.28074	-1.4033	-1.18498	-1.43614
0.6	-1.52797	-1.40419	-1.4038	-1.28136	-1.5572	-1.99296	-1.69374	-1.81792	-1.81973	-1.9418	-1.73398	-2.12234
0.8	-2.06428	-1.94046	-1.9418	-1.81971	-2.10515	-2.6786	-2.23136	-2.35616	-2.35913	-2.4796	-2.28315	-2.80866
1	-2.60049	-2.47744	-2.48358	-2.36212	-2.653	-3.36433	-2.76913	-2.89426	-2.89857	-3.0156	-2.83246	-3.49509
1.2	-3.13661	-3.0158	-3.03185	-2.91144	-3.2008	-4.05027	-3.30705	-3.43186	-3.43735	-3.5482	-3.38189	-4.1816
1.4	-3.67272	-3.55641	-3.58996	-3.47122	-3.74862	-4.73658	-3.84509	-3.96846	-3.97454	-4.0751	-3.93141	-4.86814
1.6	-4.20886	-4.1003	-4.16192	-4.0457	-4.29653	-5.42345	-4.3832	-4.50342	-4.50889	-4.5938	-4.48099	-5.55463
1.8	-4.74512	-4.64866	-4.7524	-4.63983	-4.8446	-6.11108	-4.92136	-5.03601	-5.03888	-5.101	-5.03058	-6.24099
2	-5.28157	-5.20285	-5.36675	-5.25925	-5.39295	-6.79974	-5.45952	-5.56538	-5.56268	-5.5932	-5.58011	-6.92709

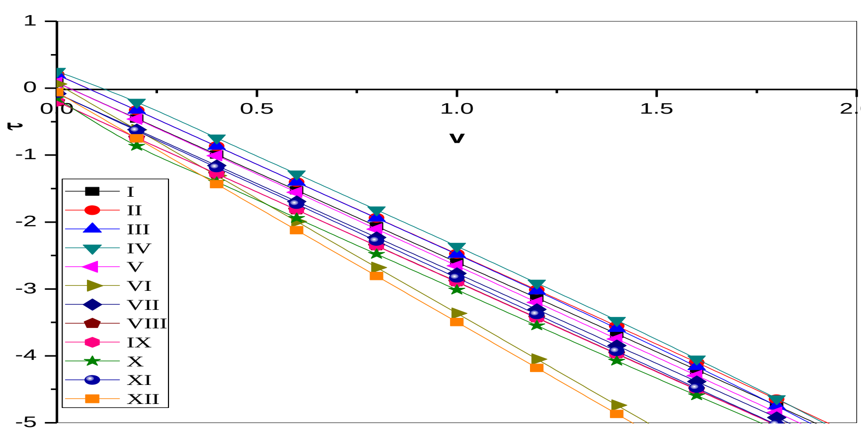

Fig 11: Skin friction at the plates *y*=0 and *y*=1: *P*=7.

Table.16: Rate of heat transfer coefficient at the plates *y*=0 and *y*=1: *P*=0.71.

v	I	II	III	IV	V	VI	VII	VIII	IX	X	XI	XII
0	-0.00740	-0.00735	-0.00586	-0.00895	-0.00483	-0.00593	-0.00598	-0.00743	-0.00602	-0.0092	-0.00484	-0.0066
0.2	0.00052	0.00041	0.00081	0.00033	0.00043	0.00058	-0.00061	-0.00090	-0.00181	-0.0013	-0.00058	-0.00081
0.4	0.00226	0.00213	0.00418	0.00204	0.00192	0.00251	-0.00246	-0.00347	-0.00692	-0.0046	-0.00236	-0.00404

0.6	0.00514	0.00511	0.00992	0.00512	0.0044	0.0058	-0.00595	-0.00861	-0.01713	-0.0115	-0.00578	-0.01112
0.8	0.0092	0.00942	0.01807	0.00963	0.00794	0.01055	-0.01137	-0.01701	-0.03376	-0.0231	-0.01116	-0.02339
1	0.01449	0.01513	0.02853	0.01559	0.01258	0.01684	-0.01899	-0.02937	-0.05811	-0.0403	-0.01881	-0.04222
1.2	0.02105	0.02225	0.04115	0.02294	0.01835	0.0247	-0.02911	-0.04636	-0.09145	-0.0644	-0.02905	-0.06897
1.4	0.02889	0.03079	0.05567	0.03159	0.02528	0.03418	-0.042	-0.06866	-0.13501	-0.0963	-0.0422	-0.10503
1.6	0.03805	0.04073	0.07176	0.04136	0.03341	0.04528	-0.05793	-0.09694	-0.18999	-0.137	-0.05857	-0.15179
1.8	0.04854	0.05203	0.08897	0.05205	0.04275	0.05799	-0.07719	-0.13185	-0.25756	-0.1875	-0.07848	-0.21063
2	0.0604	0.06464	0.10679	0.06337	0.05332	0.07227	-0.10005	-0.17404	-0.33886	-0.2489	-0.10223	-0.28298

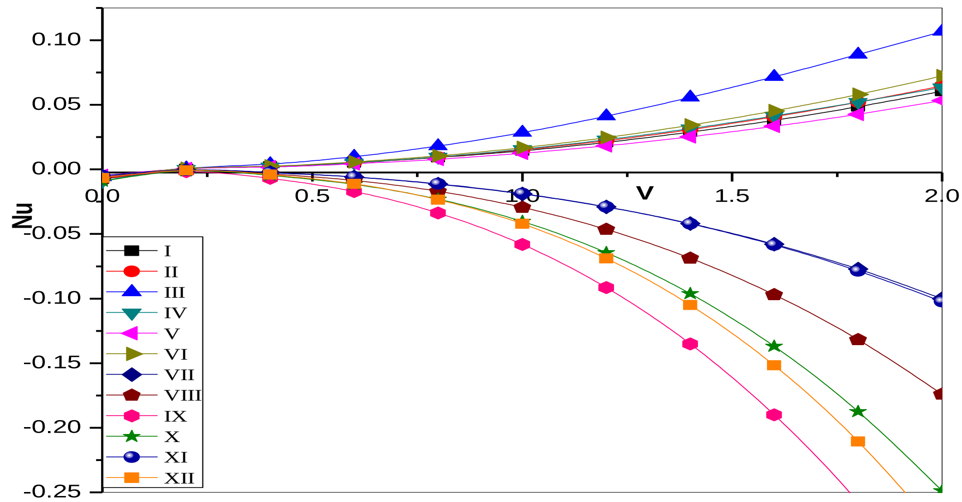

Fig 12: Rate of heat transfer coefficient at the plates y=0 and y=1: P=0.71.

Table.17: Rate of heat transfer coefficient at the plates y=0 and y=1: P=7.

v	I	II	III	IV	V	VI	VII	VIII	IX	X	XI	XII
0	-0.0253	-0.02725	-0.05663	-0.76662	-0.21955	-0.02533	-0.02876	-0.02803	-0.05818	-0.7686	-0.21968	-0.02539
0.2	0.00502	0.00381	0.00712	0.00299	0.00456	0.00544	-0.00601	-0.00877	-0.01705	-0.0119	-0.00572	-0.00819
0.4	0.0211	0.0179	0.0294	0.0149	0.0193	0.0215	-0.0241	-0.03304	-0.06173	-0.0423	-0.02319	-0.04132
0.6	0.0468	0.03799	0.0496	0.02675	0.04286	0.04448	-0.0578	-0.07959	-0.13904	-0.1005	-0.05621	-0.11484
0.8	0.08128	0.05902	0.04421	0.02559	0.07429	0.06958	-0.10913	-0.15163	-0.24224	-0.1887	-0.10717	-0.244
1	0.12345	0.07361	-0.02071	-0.0076	0.11237	0.08984	-0.17992	-0.25129	-0.35876	-0.3065	-0.17831	-0.44485
1.2	0.17185	0.07201	-0.18962	-0.09796	0.15542	0.09626	-0.27187	-0.37961	-0.47018	-0.4505	-0.27166	-0.73422
1.4	0.22458	0.04207	-0.51749	-0.27668	0.20128	0.07771	-0.38644	-0.53655	-0.55226	-0.6148	-0.38908	-1.12973
1.6	0.2794	-0.03072	-1.06978	-0.58104	0.24741	0.02098	-0.52497	-0.72096	-0.57495	-0.7905	-0.53224	-1.64978
1.8	0.33369	-0.16325	-1.92248	-1.05441	0.29079	-0.08923	-0.68861	-0.93065	-0.50234	-0.966	-0.70264	-2.31357
2	0.38443	-0.3748	-3.16207	-1.74625	0.32798	-0.27032	-0.87833	-1.16229	-0.29271	-1.1269	-0.90159	-3.14109

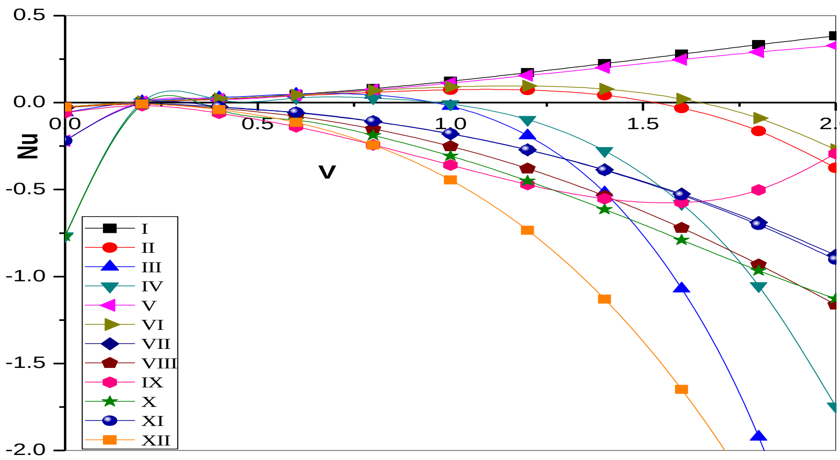

Fig 13: Rate of heat transfer coefficient at the plates y=0 and y=1: P=7.